Society For Biomaterials

IO_4^--stimulated crosslinking of catechol-conjugated hydroxyethyl chitosan as a tissue adhesive

Xiaoting Peng,[1] Yanfei Peng,[1] Baoqin Han,[1] Wanshun Liu,[1] Fuming Zhang,[2,3,4,5] Robert J Linhardt[2,3,4,5]

[1]College of Marine Life Sciences, Ocean University of China, Qingdao, China
[2]Department of Chemistry and Chemical Biology, Center for Biotechnology and Interdisciplinary Studies, Rensselaer Polytechnic Institute, Troy, New York 12180
[3]Department of Chemical and Biological Engineering, Center for Biotechnology and Interdisciplinary Studies, Rensselaer Polytechnic Institute, Troy, New York 12180
[4]Department of Biology, Center for Biotechnology and Interdisciplinary Studies, Rensselaer Polytechnic Institute, Troy, New York 12180
[5]Department of Biomedical Engineering, Center for Biotechnology and Interdisciplinary Studies, Rensselaer Polytechnic Institute, Troy, New York 12180

Received 27 September 2017; revised 26 February 2018; accepted 17 April 2018
Published online 7 May 2018 in Wiley Online Library (wileyonlinelibrary.com). DOI: 10.1002/jbm.b.34150

Abstract: Catechol-functionalized polymers are of particular interest because of their strong water-resistant adhesive properties. Hydroxymethyl chitosan (HECTS) has been used as an implantable biomaterial having good water solubility, biodegradability and biocompatibility. Here, hydrocaffeic acid (HCA) grafted HECTS (HCA-*g*-HECTS) was prepared through carbodiimide coupling and the tethered catechol underwent periodate (IO_4^-)-stimulated mono and double cross-linking with genipin. The gelation time of these cross-linked HCA-*g*-HECTS hydrogels decreased with increasing molar ratio of cross-linker to grafted catechol group, increasing temperature, or the addition of genipin. Under the same molar ratio of cross-linker to catechol, IO_4^--induced cross-linked HCA-*g*-HECTS hydrogels exhibited much stronger storage modulus and temperature stability than hydrogels made by Fe^{3+}-triggered cross-linking. The IO_4^--stimulated HCA-*g*-HECTS hydrogels were biocompatible on a cellular level when the molar ratio of IO_4^- to catechol group was less than 0.5:1. The hydrogels prepared with a 0.125:1 molar ratio of IO_4^- to catechol group exhibited high adhesion strength of 73.56 kPa against wet rat skin, and a higher adhesion strength than sutures in a rat wound closure model. This biocompatible IO_4^--stimulated HCA-*g*-HECTS hydrogel may represent a promising new tissue adhesive. © 2018 Wiley Periodicals, Inc. J Biomed Mater Res Part B: Appl Biomater 107B: 582–593, 2019.

Key Words: hydroxyethyl chitosan, catechol group, hydrogel, tissue adhesive

How to cite this article: Peng X, Peng Y, Han B, Liu W, Zhang F, Linhardt RJ. 2019. IO4–-stimulated crosslinking of catecholconjugated hydroxyethyl chitosan as a tissue adhesive. J Biomed Mater Res Part B 2019:107B:582–593.

INTRODUCTION

In nature, mussels are found clumped together with each attached to wave washed rocks through its byssus. The expanded plaques at the distal ends of these threads bind to the rock's foreign surface. The adhesive in these plaques must be rapid setting, strong and tough, or else the mussel will be dislodged by waves. Biochemical analysis reveal the existence of dozens of proteins within the byssus. Those confined to mussel plaques are mussel foot proteins (mfp) that include mfp-2, mfp-3, mfp-4, mfp-5 and mfp-6.[1] The secret behind a mussels' adhesive is a rare amino acid called dihydroxyphenylalamine (DOPA).[2] Mfp-3 and mfp-5 in the interfacial region between the plaque and the substratum contain high amount of DOPA.[3–6] Recent research suggests that the reduced catechol form of DOPA binds directly to surfaces, and oxidized states of DOPA, that is, the simiquinone and quinone, regain surface-binding ability after being reduced.[7–10] The cohesion with mfps may be brought about through metal ion templating and redox chemistry.[11–14]

Due to the unique adhesive performance of mfps in wet and turbulent environments, mfps have been the targets for biomimetics.[15–17] Typically, polymers are chemically derivatized with catechols in the form of DOPA or DOPA mimetic functional groups, such as 3,4-dihydroxyhydrocinnamic acid (hydrocaffeic acid, HCA) and 3,4-dihydroxybenzealdehyde.[18,19] Catechol-conjugated polymers, including poly(ethylene glycols) (PEG–catechol), hyaluronic acid (HA–catechol), alginate (Alg–catechol), heparin (Hep–catechol), dextran (Dex–catechol) and chitosan (Chi–catechol), have recently been reported.[20–28]

Correspondence to: Y. Peng; e-mail: yanfeipeng@ouc.edu.cn
Contract grant sponsor: National Key R&D Program of Shandong Province; contract grant number: 2016GSF115003 (China Scholarship Council)

Chitosan, a polysaccharide obtained by partial deacetylation of naturally occurring chitin, has been used in numerous biomedical applications, including wound dressings, hemostatic materials, drug/gene delivery depots and tissue engineering scaffolds.[29] Various preparation methods, characteristics and biomedical applications of chitosan–catechol have been reported.[30–36] Chitosan–catechol exhibits excellent solubility at neutral pH solutions and strong adhesiveness to tissue surfaces. HCA has been conjugated to amino groups in the chitosan backbone through carbodiimide coupling. Some chitosan–catechol products have been reported with a degree of catechol conjugation (DOcC) value of 4–30 mol % and even up to 82 mol % for 7-day reactions. Catechol conjugation also enhances the water-solubility of chitosan at a neutral pH, for example, catechol-chitosan with a DOcC of 7.2 mol % has a solubility of ~63 mg/mL at pH 7.0.[37,38] Reductive amination between the amino groups of chitosan and an aldehyde-terminated catechol represents another approach for the preparation of catechol-chitosan with high DOcC using a short reaction time. The main drawback of catechol-chitosan obtained by reductive amination is that it can dissolve only in acid solutions limiting its application as a tissue adhesive.[12]

In our previous studies, hydroxymethyl chitosan (HECTS) has been demonstrated as an implantable biomaterial with excellent biodegradability, biocompatibility and water solubility over a pH range of 1 to 14.[39–42] In the current study, we report the preparation of HECTS based hydrocaffeic acid grafted chitosan derivative (HCA-*g*-HECTS) through IO_4^--induced gel formation. The materials ware structurally characterized and evaluated both *in vitro* and *in vivo* biocompatibilities and water-resistant adhesion.

MATERIALS AND METHODS

Materials

HECTS (96% deacetylation) was synthesized in our laboratory as previous report.[42] 3,4-dihydroxyhydrocinnamic acid (HCA), 1-ethyl-3-(3-dimethylaminopropyl)-carbodiimide hydrochloride (EDC), *N*-hydroxysulfosuccinimide sodium salt (sulfo-NHS) and 2-(*N*-morpholino) ethanesulfonic acid buffer (MES) were purchased from Sinopharm Chemical Reagent Co., Ltd (Shanghai, China). Regenerated cellulose tube (MWCO 5000 Da) was from Union Carbide (Houston, Texas).

Synthesis of HCA-*g*-HECTS

HCA-*g*-HECTS was synthesized by Bosch reduction of Schiff based on a reported method with modifications.[30] Typically, 0.55 g EDC and 0.21 g sulfo-NHS in 0.1 M MES (25 mL) were mixed with 0.17 g HCA in 25 mL ethanol. The solution was added quickly to 2% HECTS in hydrochloric acid (pH 5.5, 50 mL) with intensive stirring for 48 h. The reaction was stopped by dialysis against acidified distilled water (pH 5.0) for 2 days followed by distilled water for 12 h. The final product was lyophilized to give a white HCA-*g*-HECTS powder and kept in a moisture-free desiccator.

Structural characterization of HCA-*g*-HECTS

UV–Vis absorption was recorded with Tu-1800 UV-Vis spectrophotometer (PGeneral, China). The infrared spectra were recorded on Nicolet NEXUE470 FTIR (Thermo Fisher Scientific Waltham, MA) in a range of 400–4000 cm^{-1}. The heterogeneity and molecular weight of HCA-*g*-HECTS were determined using a SHIMADZU HPLC system (Kyoto, Japan) equipped with a Shodex OHpak SB-804M HQ column (8.0 mm ID × 30.0 cm), SPD-10A detector (280 nm) and refractive index detector (RID). The mobile phase was 0.1 mol/L Na_2SO_4 with a flow rate of 0.5 mL/min at 30°C. Data were processed by ClassVP software. The molecular weight was estimated according to a calibration curve of dextran standards. Proton nuclear magnetic resonance spectroscopy (^{1}H NMR) was recorded with a Bruker Avance III 600 MHz spectrometer (Germany) fitted with a 5 mm TCI-cryo probe at 25°C, operating at 600 MHz. Sample (30 mg) was dissolved in D_2O (99.8%, 0.6 mL). Chemical shifts are given in ppm using acetone as an internal standard at 2.05 ppm for ^{1}H NMR. The degree of HCA conjugation was calculated by dividing the integration value of the catechol proton peaks that appeared from 6.5 to 6.7 ppm by the value of the acetyl group protons from 1.9 to 1.93 ppm multiplied by 11 because the degree of acetylation of HECTS was determined to be 9%.[37]

Crosslinking of HCA-*g*-HECTS by IO_4^-

The HCA-*g*-HECTS was firstly dissolved in distilled water to a concentration of 13 wt %. Then 8, 12, and 16 mg/mL $NaIO_4$ in distilled water was added to 1.0 mL of HCA-*g*-HECTS solution to make the molar ratio of IO_4^- to HCA as 0.4:1, 0.7:1 and 1:1, respectively, and mixed to form IO_4^--stimulated HCA-*g*-HECTS hydrogel (IO_4^-- HCA-*g*-HECTS). Double crosslinking of HCA-*g*-HECTS was performed as described by Fan et al.with modification.[43] Briefly, genipin was added to HCA-*g*-HECTS solution and stirred to make a homogeneous solution, followed by the addition $NaIO_4$. The exact preparation conditions for G-IO_4^--HCA-*g*-HECTS hydrogel including rheological time-sweep measurement, rheological frequency-sweep measurement, and swelling measurement are provided in Table I.

As comparison, Fe^{3+} triggered HCA-*g*-HECTS hydrogel (Fe^{3+}-HCA-*g*-HECTS) was performed similarly except for replacing $NaIO_4$ with 6 mg/mL, 8 mg/mL and 12 mg/mL $FeCl_3$ in distilled water. Double crosslinking of Fe^{3+}-HCA-*g*-HECTS by genipin was achieved similarly as G-IO_4^--HCA-*g*-HECTS hydrogel.

Rheological measurement

Rheological properties were tested by using a DHR-1 rheometer (TA Instruments, New Castle, DE) equipped with 20 mm diameter stainless steel parallel plate geometry at 25°C and 37°C. The gap between the stainless steel parallel plate geometry and the base plate was 1.0 mm for all tests. Dynamic strain sweep was conducted prior to the frequency sweep, and the strain was determined to be 1% to ensure the rheological measurements were within a linear viscoelastic range. The storage modulus (G′) and loss modulus (G″) were determined with frequency sweeps between 0.01 and 100 rad/s. The gelation time was measured by carrying out time sweeps, the frequency and strain was set at 1.0 rad/s and 1%, respectively. The tests were started as soon

TABLE I. Preparation of Double Cross-Linked G-IO_4^--HCA-*g*-HECTS hydrogels

Experiments	HCA-*g*-HECTS in Distilled Water (wt %, μL)	0.2% Genipin in 70% Ethanol (μL)	G-IO_4^--HCA-*g*-HECTS	
			Concentration and Vof $NaIO_4$ (mg/mL, μL)	Molar Ratio of IO_4^- to HCA
Time-sweep rheology	13, 100	20	8, 100	0.4:1
Frequency-sweep rheology	13, 100	20	8, 100	0.4:1
Swelling	15, 100	20	6.5, 25	0.125:1
Wet-resistant adhesion	15, 100	20	6.5, 25	0.125:1
Cytotoxity and rat skin closure	15, 100	20	6.5, 25	0.125:1

as the addition of $NaIO_4$ (or $FeCl_3$) solution. Each test was replicated three times.

Swelling measurement

IO_4^--HCA-*g*-HECTS hydrogels with the molar ratio of $NaIO_4$ to HCA to be 0.5:1, 0.25:1, 0.125:1, and 0.0625:1 were prepared by adding $NaIO_4$ solution (6.5 mg/mL, 100 μL, 50, 25 and 12.5 μL, respectively) into 100 μL of HCA-*g*-HECTS solution (15 wt %). Double crosslinking of HCA-*g*-HECTS hydrogels with the molar ratio of $NaIO_4$ to HCA as 0.0625:1 were formed as described in Table I. All hydrogels were weighed to obtain the initial mass (W_0) and equilibrated mass (W_1) after being immersed in distilled water for 24 h. The swelling percentage was calculated with the Equation (1) and data were expressed as means ± SEM based on 5 tests per sample.

$$\text{Swelling } (\%) = \frac{(W_1 - W_0)}{(W_0)} \times 100\% \quad (1)$$

Wet-resistant adhesion strength measurement

The adhesive properties of IO_4^--stimulated HCA-*g*-HECTS hydrogels were evaluated by lap shear tests utilizing a SHIMADZU AGS-X 500 N tensile mechanical tester (Kyoto, Japan) as reported with modification.[44–46] Rat skin samples from sacrificed Sprague-Dawley rats were barbered and cut into 4.0 cm × 1.5 cm rectangular strips. The outside skin then adhered to a PTFE board by cyanoacrylate glue, and immersed in physiological salt solution to ensure it moist before use. HCA-*g*-HECTS hydrogels (100 μL) were then applied evenly to the inner skin with an area of 1.5 cm × 1.5 cm, where another skin was covered quickly and kept at room temperature for 2 h and 24 h in a highly humid chamber. The adhesion strength was obtained by dividing the maximum load by the corresponding overlapping area. The tests were implemented at a tensile rate of 5 mm/min. Three samples from each hydrogel were tested.

Cytotoxicity of HCA-*g*-HECTS and IO_4^--stimulated-HCA-*g*-HECTS hydrogels

Co-irradiation sterilized HECTS or HCA-*g*-HECTS (2.0 mg/mL) were dissolved in Dulbecco's modified eagle's media (DMEM) containing 10% (v/v) fetal bovine serum (FBS) and 1% (v/v) penicillin/streptomycin (100 IU/mL), which was sterilized by 0.2 μm membrane filtration. Mouse fibroblast L929 cells were cultured in DMEM at 37°C in a humidified atmosphere with 5% CO_2. Cells at a density of 1.8×10^4 cells/mL were then seeded in 96-well plates with 200 μL/well, and cultured in the incubator for 24 h. The culture media were then replaced with 200 μL fresh DMEM media, HECTS or HCA-*g*-HECTS solution, and the plates were then incubated at 37°C in a humidified atmosphere with 5% CO_2 for 24 and 48 h, respectively. The viability of cells was determined by 3-(4,5-dimethyl-2-thiazolyl)-2,5-diphenyl-2-H-tetrazolium bromide (MTT) assay. The cell relative growth ratio (RGR) was calculated as following equation:

$$\text{RGR } (\%) = \frac{(OD_1 - OD_0)}{(OD_2 - OD_0)} \times 100\% \quad (2)$$

where OD_0, OD_1 and OD_2 were the average optical density (OD) of the blank, sample (either HECTS or HCA-*g*-HECTS) and negative control groups, respectively. For each sample 6 wells were used in parallel. Experiments were performed in triplicate.

Following ISO standard 100993-5, the cytotoxicity of IO_4^--stimulated-HCA-*g*-HECTS hydrogels was also evaluated by using extract tests. First, IO_4^--stimulated-HCA-*g*-HECTS hydrogels were formed by addition of different concentrations of sterile $NaIO_4$ solutions to 100 μL HCA-*g*-HECTS solution (15 wt %), sterilized by dissolving Co irradiation sterilization HCA-*g*-HECTS in sterilized distilled water) with the molar ratio of $NaIO_4$ to HCA to be 0.5:1, 0.25:1, 0.125:1 and 0.0625:1. The hydrogels were then immersed in 8 mL DMEM containing FBS and penicillin/streptomycin for 24 h at 37°C under 100 rpm followed by filtration against 0.2 μm membrane to get the extract solution. L929 cell seeded in 96-well plates was then treated by the extract solution for 24 h and 48 h and evaluated as described above.

***In vivo* biocompatibility and biodegradability of IO_4^--stimulated-HCA-*g*-HECTS hydrogels**

The animal experiments in present study were carried out in accordance with the ethical guidelines of the Shandong Province Experimental Animal Management Committee and were in complete compliance with the National Institutes of Health Guide for the Care and Use of Laboratory Animals. Twenty adult male Sprague-Dawley rats (weight, 200 ± 10 g) were housed in individual cages and kept under controlled temperature and humidity with free access to food

and water. Four rats were normally raised as a control. Sixteen rats were then anesthetized with intraperitoneal administration of pentobarbital sodium (3% in normal saline) at a dose of 1 mL/kg. The dorsal sides of the rats were gently shaved and disinfected with 75% of alcohol. IO_4^--stimulated-HCA-*g*-HECTS hydrogel (100 μL, with a molar ratio of $NaIO_4$ to HCA of 0.125:1), prepared with irradiation sterilized HCA-*g*-HECTS and filtered through a 0.2 μm membrane was implanted into the dorsal skeletal muscle and the subcutis of eight rats. G-IO_4^--stimulated-HCA-*g*-HECTS hydrogels (100 μL with a molar ratio of $NaIO_4$ to HCA of 0.125:1, double cross-linked with 20 μL genipin) was similarly implanted. On the 3rd day and the 7th day after the surgery, four rats of each gel group were sacrificed, the muscles and skin at the injection sites were photographed, collected, fixed in 4% formalin, embedded in paraffin, and after hematoxylin and eosin (H&E) staining the 5 μm thick tissue sections were visualized.

In vivo wound closure by IO_4^--stimulated-HCA-*g*-HECTS hydrogels

Based on the *in vitro* lap shear testing, IO_4^--stimulated-HCA-g-HECTS hydrogels (with the molar ratio of $NaIO_4$/HCA to be 0.125:1) and G-IO_4^--HCA-g-HECTS hydrogel double cross-linked with genipin were selected for *in vivo* wound closure evaluation.[44] After anesthetization and sterilization of the rat skin, 2 full-thickness wounds (2 cm long × 0.5 cm deep) were made on the dorsum of each Sprague–Dawley rats (female, average weight of 300 ± 50 g). One wound on each rat was closed by dropping 100 μL of sterilized IO_4^--HCA-g-HECTS hydrogel (four rats) or G-IO_4^{-1}-HCA-g-HECTS hydrogel (four rats) into the wound followed by waiting for about 2 min. The other wounds were closed by conventional suturing as the control. At two days post-wounding, the test animals were sacrificed and skin tissues at wound sites were excised for histological analyses. These sections were stained with H&E for morphological assessment. The wound closure was evaluated by measuring the tensile mechanical strength of the tissues at the incision site.

Statistical analysis

Experimental data in present study was expressed as mean ± standard derivation. Statistical analysis of data was performed by one-way ANOVA on SPSS (VERSION 20.0). The statistical significance was evaluated by Student's *t* test, with $p < 0.05$ as the minimal level of significance.

RESULTS

Synthesis and characterization of HCA-HECTS conjugates

Crosslinking primary amines to carboxylic acid groups by using EDC is a powerful and versatile tool for bioconjugation, which has been used successfully for preparing water-soluble hydrocaffeic acid (HCA) branched chitosan.[30] Based on the fewer unsubstituted NH_2 groups in hydroxyethyl chitosan (HECTS) than found in the original chitosan, EDC/sulfo-NHS was applied for the synthesis of HCA grafted HECTS (HCA-*g*-HECTS) in this study. The synthetic scheme is illustrated in Figure 1(A). HPLC chromatogram of HCA-*g*-HECTS shows a symmetric peak in both UV_{280nm} and RID detectors, demonstrating that HCA had been conjugated to HECTS [Figure 1(B)]. In comparison with the FTIR spectrum of HECTS, new absorption peaks at 2712 cm^{-1} and 1600 cm^{-1} appeared in the HCA-*g*-HECTS spectrum due to aromatic and aliphatic C=O stretching, further demonstrating the successful conjugation of HCA to HECTS [Figure 1(C)].[32] The ^1H NMR spectra [Figure 1(D)] exhibit signals at δ 6.6–6.8 ppm arising from the aromatic ring protons of catechol group of HCA- *g*-HECTS. The degree of HCA conjugation reached to 14.8% using the optimized reaction conditions, a molar ratio of EDC:sulfo-NHS:HCA:HECTS: 3:1:1:5 at pH 5.5 with a reaction time of 3 days.

IO_4^- stimulated HCA-HECTS hydrogels formation

Cross-linking of HCA-*g*-HECTS can be achieved by addition of oxidants, such as sodium periodate. The catechol group can be, thus, oxidized to be highly reactive quinone that is capable of intermolecular cross-linking. To compare periodate cross-linked hydrogels with Fe^{3+} mediated HCA-*g*-HECTS hydrogels (Fe^{3+}- HCA-*g*-HECTS), which could coordinate theoretically all three catechol groups, molar ratios of 0.4:1, 0.7:1 and 1:1 (IO_4^- to catechol groups in HCA-*g*-HECTS) were selected to form the $NaIO_4$ triggered HCA-*g*-HECTS hydrogels (IO_4^--HCA-g-HECTS). The color of the three hydrogels prepared using three different molar ratios of IO_4^- to catechol groups were yellow, light brown, and brown, respectively. As shown in Table II, the gelation time of IO_4^--HCA-*g*-HECTS began much sooner with the increased molar ratio of IO_4^- to catechol group in HCA-HECTS. When the molar ratio of IO_4^- to catechol group increased from 0.4:1 to 1:1, the time for gel formation decreased from 281 s to 79 s. By changing the gelation temperature from 25°C to 37°C the gelation occurred more quickly. Thus, the gelation time of IO_4^--HCA-*g*-HECTS was dependent on the molar ratio of IO_4^- to catechol group and gelation temperature. Genipin is a biocompatible cross-linker that can spontaneously react with the primary amino group of HECTS. Double cross-linking with genipin resulted in a much quicker gelation of HCA-*g*-HECTS than did single cross-linking. After adding genipin, the gelation time of IO_4^- stimulated HCA-*g*-HECTS hydrogel at 37°C was <20 s (Table II).

Dynamic rheology properties of IO_4^--HCA-*g*-HECTS hydrogels

The viscoelastic properties of HCA-*g*-HECTS hydrogels were determined using oscillatory rheometry. The frequency sweep of HCA-*g*-HECTS by IO_4^-, triggered gelation at different molar ratio of IO_4^- to catechol group is illustrated in Figure 2(A). At each molar ratio of IO_4^- to catechol group, the formed hydrogel exhibited typical features of a chemically cross-linked elastic polymer with a frequency-independent behavior and a higher storage modulus (G′) than loss modulus (G″). A higher G′ was obtained by increasing the molar ratio of IO_4^- to catechol groups. When the molar ratio of IO_4^- to catechol groups was 1:1, the G′ reached 60 Pa, a value ten-times higher than that of Fe^{3+}-HCA-*g*-HECTS at the same molar ratio of cross-

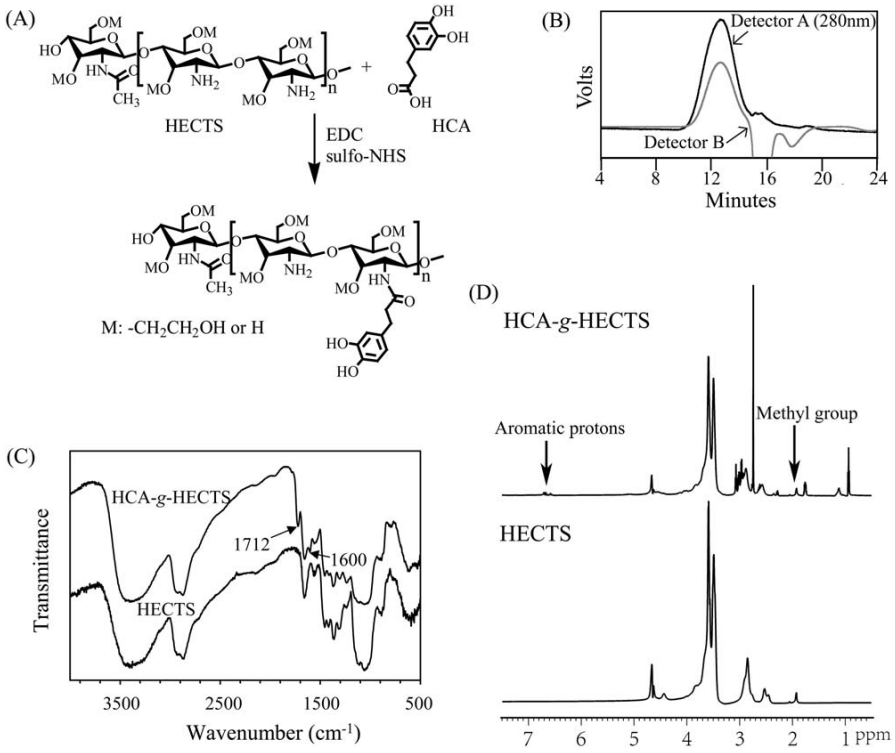

FIGURE 1. Structural characterizationof HCA-*g*-HECTS. Synthetic scheme (A), HPLC of HCA-*g*-HECTS (DOC = 14.8%) detected by UV 280 nm and RID (B), FTIR spectra of HECTS and HCA-*g*-HECTS (DOC = 14.8%) with the major absorbance for the functional group noted (C) and ^{1}H NMR spectra of HECTS and HCA-*g*-HECTS (DOC = 14.8%) in D_2O at 25°C with acetone as an internal standard (D).

linker to catechol groups [Figure 2(D)]. As the temperature increased from 25 to 37°C, both G′ and G″ of IO_4^--HCA-*g*-HECTS showed no obvious change [Figure 2(B)]. These results suggest that IO_4^--HCA-*g*-HECTS is both highly stable and uniform. After double crosslinking of IO_4^--HCA-*g*-HECTS (IO_4^- to catechol group was 0.4:1) with genipin, G′ and G″ were hundreds of times stronger than that of the IO_4^- cross-linked hydrogels [Figure 2(C)]. Considering the much shorter gelation time by adding genipin (as listed in Table I), double cross-linking with genipin provides a potentially biocompatible way to decrease the concentration of IO_4^- while keeping the strength needed of IO_4^--HCA-*g*-HECTS hydrogel.

The Fe^{3+}-HCA-*g*-HECTS hydrogel shows behavior of both a non-covalent cross-linking and a covalent cross-linked elastic, with both temperature sensitivity and a much lower G′ than IO_4^--HCA-*g*-HECTS hydrogels [Figure 2(D–F)]. The double cross-linked genipin (G-Fe^{3+}-HCA-*g*-HECTS) hydrogels had both G′ and G″ values significantly higher than those of Fe^{3+}-HCA-*g*-HECTS in a frequency-independent manner [Figure 2(F)].

Swelling of HCA-HECTS hydrogels

The swelling property of a hydrogel is important for both mass transfer and cellular function properties.[47] The degree of equilibrium swelling for a hydrogel depends on the cross-link and charge densities of its polymer network. The swelling ratios of HCA-HECTS hydrogels were calculated by measuring the change of the weight of hydrogels in distilled water at 37°C. Swelling studies indicated that equilibrium swelling of the hydrogel composites had been reached after being immersed in distilled water overnight (data not shown). The swelling of IO_4^--HCA-*g*-HECTS was studied as a function of the molar ratio of IO_4^- to catechol group (Figure 3). The degree of swelling of HCA-*g*-HECTS hydrogels decreased with an increase of IO_4^- to catechol group, suggesting an increased cross-linking of the hydrogel. Keeping the molar ratio of IO_4^- to catechol as 1:0.0625, double cross-linking with genipin could decrease the swelling of IO_4^--HCA-*g*-HECTS hydrogel.

Water resistant adhesion

The lap shear tensile strength of HCA-*g*-HECTS and its hydrogels gluing onto wet rat skin is provided in Table III.

TABLE II. Gelation Point of HCA-*g*-HECTS Hydrogels

Crosslinker	Cross-Linker to HCA (Molar Ratio)	Gelation Point (s) at 25°C	Gelation Time at 37°C (s)
IO_4^-	0.4:1	281	220
	0. 7:1	144	90
	1:1	79	<20
G/IO_4^-[a]		21	<20

[a] Double cross-linking of IO_4^- stimulated HCA-*g*-HECTS (molar ratio of IO_4^- to HCA was 0.4:1).

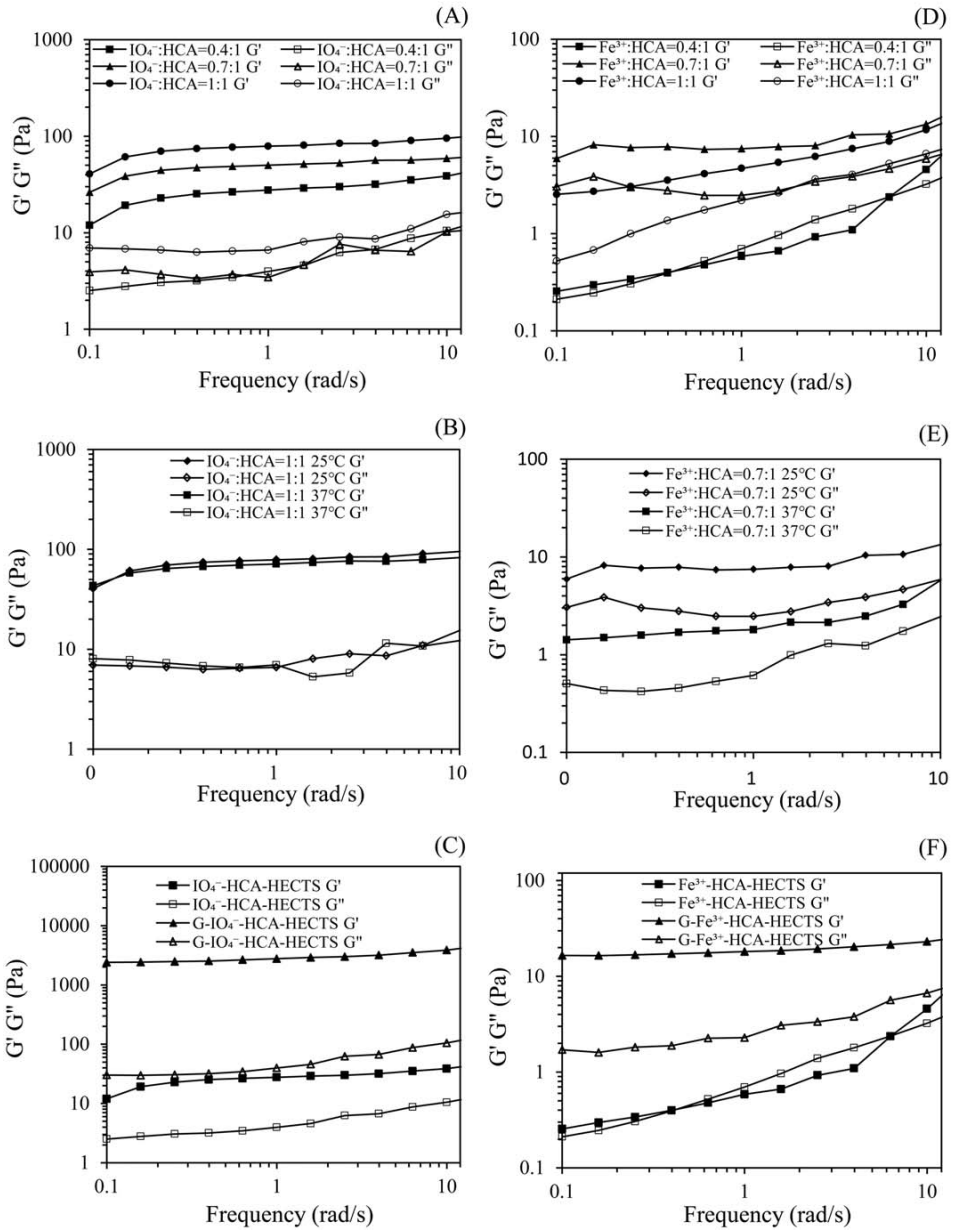

FIGURE 2. Rheology analysis (frequency sweep) of HCA-HECTS hydrogel. Storage modulus (*G*′) and loss modulus (*G*″) of IO_4^- stimulated HCA-*g*-HECTS hydrogels formed (A) in different molar ratio of Fe^{3+} or IO_4^- to HCA at 25°C, (B) at different gelation temperature (IO_4^- to HCA was 1:1), and (C) double cross-linking with genipin (IO_4^- to HCA was 0.4:1). For comparison, the rheology analysis of Fe^{3+} triggered HCA-*g*-HECTS hydrogels were shown in (D–F). Storage modulus (*G*′) and loss modulus (*G*″) of Fe^{3+} triggered HCA-*g*-HECTS hydrogels formed (D) in different molar ratio of $Fe^{3+}$to HCA at 25°C, (E) at different gelation temperature (Fe^{3+} to HCA was 0.4:1), and (F) double cross-linking with genipin as a second cross-linker (Fe^{3+} to HCA was 0.4:1).

The adhesion strength is highly dependent on the overlapping time and the formulation to form the hydrogels. After overlapping for 15 min, IO_4^--HCA-*g*-HECTS, at a molar ratio of IO_4^- to catechol group at 0.25:1, slightly improved adhesion strength as compared with that of pure HCA-*g*-HECTS. There was also no significant difference in adhesion strength among the three IO_4^--HCA-*g*-HECTS hydrogels prepared from the molar ratio of IO_4^- to catechol group as 0.125:1, 0.25:1 and 0.5:1. When the overlapping time reached to 24 h, the adhesion strength of both HCA-*g*-HECTS and IO_4^--HCA-*g*-HECTS clearly increased. The adhesion strength of IO_4^--HCA-*g*-HECTS under the molar ratio of IO_4^- to catechol group at 0.125:1 showed the highest value of 73.56 kPa, increasing over 70-times as compared to the hydrogel overlapped for 15 min, suggesting that the conjugation of IO_4^--HCA-*g*-HECTS to skin occurs much more

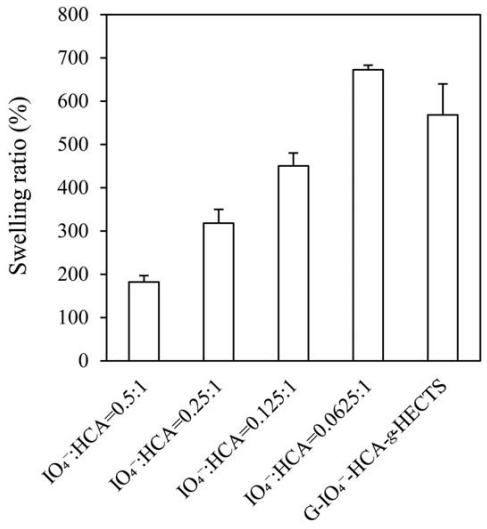

FIGURE 3. Swelling ratio of IO_4^- stimulated HCA-*g*-HECTS hydrogels in different molar ratio of IO_4^- to HCA at 25°C. G- IO_4^- corresponded to IO_4^- stimulated HCA-*g*-HECTS hydrogel with the molar ratio of IO_4^- to HCA as 0.0625:1 that was further cross-linked with genipin.

slowly than does the formation of hydrogel. As expected, the adhesion strength increased with the decreasing molar ratio of IO_4^- to catechol group, since IO_4^- was required to form the hydrogel but IO_4^- also consumed catechol groups that were responsible for tissue adhesion. It is noteworthy that the adhesion strengths of IO_4^--HCA-*g*-HECTS, at molar ratios of IO_4^- to catechol group as 0.5:1 and 0.25:1, were higher than that of HCA-*g*-HECTS free from cross-linker. Keeping the molar ratio of IO_4^- to catechol group at 0.125:1, double cross-linking IO_4^--HCA-*g*-HECTS with genipin slightly decreased the adhesion strength.

Cytotoxicity of HCA-*g*-HECTS conjugates and HCA-*g*-HECTS hydrogels

Quantitative MTT assay was used to evaluate the cytotoxicity of HECTS, HCA-*g*-HECTS by DMEM cell culture medium on L929 cells after one day and two days of culture. Neither HECTS nor HCA-*g*-HECTS in the concentration from 0.0625 mg/mL to 2.0 mg/mL inhibited the proliferation of L929 cells, suggesting that they were nontoxic on a cellular level [Figure 4(A,B)].

There are reports on the good biocompatibility of Fe^{3+}, IO_4^- and genipin induced cross-linking of catechol group conjugated polymers.[25,42] The MTT assay of the extract solution from IO_4^--HCA-HETCS hydrogels prepared with different molar ratio of IO_4^- to HCA is shown in Figure 4(C). A significant inhibition of cell growth was found when culturing in the extract solution of hydrogel with the molar ratio of IO_4^- to HCA as 1:1, while no reduction of cell growth (with a RGR exceeding 100%) appeared upon treatment with the extract solution of hydrogel with a lower molar ratio of IO_4^- to HCA. The amount of genipin used for double cross-linking IO_4^--*g*-HCA-g-HECTS also showed an effect on the cell growth. Since IO_4^--*g*-HCA-g-HECTS at a molar ratio of IO_4^- to HCA of 0.125:1 exhibited the highest adhesion strength on wet rat skin, it was further cross-linked with different volumes of 0.2% genipin. Using the three genipin volumes (10, 15 and 20 μL), hydrogel extracts were found to be noncytotoxic, with a RGR >85% [Figure 4(D)]. Based on these results, IO_4^-- HCA-*g*-HECTS prepared using molar ratio of IO_4^- to HCA of 0.125:1 and double cross-linked hydrogel with 20 μL genipin were further evaluated for *in vivo* biocompatibility

TABLE III. Lap Shear Adhesion Test Results of HCA-*g*-HECTS and Its Hydrogels Gluing on Wet Rat Skin After Overlapping for 15 min and 24 h

Material	Cross-Linker to HCA (Molar Ratio)	Adhesion Strength (kPa) 15 min	24 h
HCA-*g*-HECTS	—	0.77 ± 0.04	46.70 ± 1.95
IO_4^--HCA-*g*-HECTS	0.125:1	0.97 ± 0.09	73.56 ± 3.40
	0.25:1	1.27 ± 0.12	66.34 ± 9.70
	0.5:1	0.57 ± 0.24	51.93 ± 11.09
G/IO_4^--HCA-*g*-HECTS[a]	—		61.41 ± 2.64

[a] Double cross linking of IO_4^- stimulated HCA-*g*-HECTS with genipin (molar ratio of IO_4^- to HCA was 0.125:1). Data in the table are the mean ± SD.

In vivo biocompatibility of IO_4^- triggered HCA-*g*-HECTS hydrogels

The *in vivo* safety analysis of HCA-*g*-HECTS hydrogels was obtained by implanting the hydrogels subcutaneously or into the dorsal skeletal muscle. The surgical procedures are presented in Figure 5(E). As shown in Figure 5(A,B), the size of both implanted HCA-*g*-HECTS hydrogels became smaller on the 3rd day than the initial size of post implantation, no inflammation was observed at the implantation site in skeletal muscle. A red trace in the subcutis around the implanted IO_4^--HCA-*g*-HECTS hydrogel was observed, however, implying a slight inflammatory reaction. By day 7, the gels were partly adsorbed and tissue necrosis, hyperemia, and hemorrhaging were not observed in either the skeletal muscle or the subcutis [Figure 5(A,B)]. Histological sections of the tissue surrounding the hydrogels were examined 3 and 7 days post implantation [Figure 5(C,D)]. In contrast to normal tissue, marked accumulation of inflammatory cells in the subcutis and muscle was observed at the injection site on day 3 but these progressively decreased and become slight by day 7. Histological response in rats after implantation of HCA-g-HECTS hydrogels was summarized in Table IV based on the method and criteria described by De Jong et al.[48,49]

In vivo rat skin incision closure

In the rat skin incision model, the bleeding at the incision site in the rat skin quickly slowed by applying either IO_4^--HCA-*g*-HECTS or G-IO_4^- -HCA-*g*-HECTS hydrogels. The wound openings closed within 2 min and remained closed during the observation (until 2 days post treatment) [Figure 6(A,B)]. The histological examination of incision area [Figure 6(C)] at day 2 post treatment, with IO_4^--HCA-*g*-HECTS and

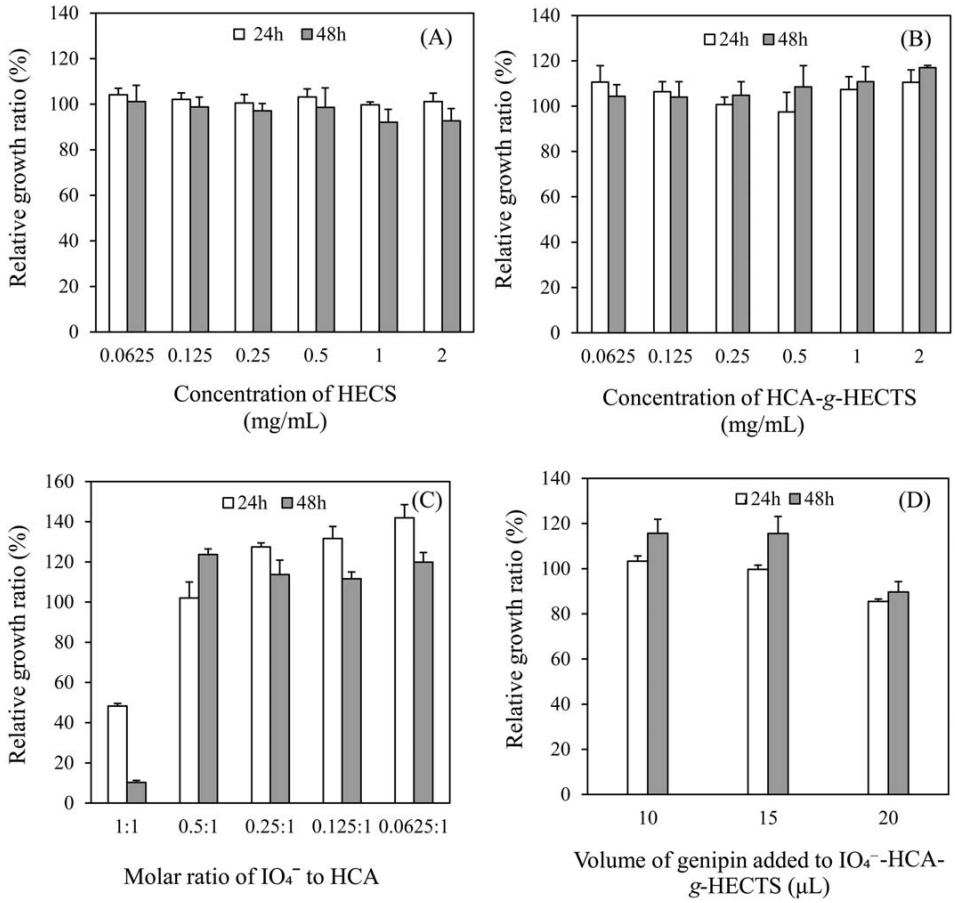

FIGURE 4. Effect of HECTS, HCA-*g*-HECTS and extract solution of HCA-*g*-HECTS hydrogels on the relative growth ratio of L292 fibroblasts on 24 and 48 h. A: HECTS, (B) HCA-*g*-HECTS, (C) extract solution of IO_4^--HCA-*g*-HECTS hydrogels with different molar ratio of IO_4^- to HCA, (D) extract solution of G-IO_4^--HCA-*g*-HECTS hydrogels with the molar ratio of IO_4^- to HCA as 0.125:1 double cross-linked with different volume of genipin.

G-IO_4^--HCA-*g*-HECTS hydrogels, showed lighter infiltrating of inflammatory cells as compared with those closed with sutures. The tensile strength of incision at 2 days post closure with IO_4^--HCA-*g*-HECTS, G-IO_4^--HCA-*g*-HECTS hydrogels and sutures is illustrated (Figure 7). Skin treated with both HCA-*g*-HECTS hydrogels had slightly higher tensile strength than suture-closed skin, and double cross-linked IO_4^--HCA-*g*-HECTS showed the highest tensile strength of 315.9 ± 66.3 kPa.

DISCUSSION

Polymers were functionalized with various catechol derivatives having strong wet-adhesive properties. Chitosan-catechol reportedly has various biomedical applications.[28] Based on their good water solubility, biodegradability and biocompatibility properties, HECTS and HCA-*g*-HECTS were prepared in this work and their wet-adhesive properties were studied. Our results showed that HCA-*g*-HECTS with a HCA conjugation degree of 14.8% exhibited excellent water-solubility (150 mg/mL in water), and good biocompatibility on cellular level even though it reportedly inhibited cell growth by reactive oxygen species released during catechol oxidation.[50]

Polymer hydrogels should adhere to tissue with sufficient mechanical strength to stay intact to effectively act as tissue adhesives.[51] Mussel-inspired, catechol-conjugated polymers can strongly bind to both inorganic and organic surfaces, and self-bond through oxidation or metal ion coordination to form cross-linked hydrogels. The consumption of catechol for cohesion has been found to diminish the catechol adhesion to mica.[11] Therefore, it's important to optimize gelation conditions while maintaining strong tissue adhesion strength.

Cross-linking of HCA-g-HECTS can be achieved by addition of oxidants such as sodium periodate. When catechol is oxidized to semiquinone or quinone, it becomes highly reactive and can participate in intermolecular covalent cross-linking and interfacial covalent bonding to the various nucleophilic functional groups (that is, $-NH_2$, –SH, imidazole) of biological substrates. The oxidative cross-linking of catechol is dependent on multiple factors including the type of oxidant, the concentration of oxidant and the pH.[20] Periodate mediated cross-linking involves the polymerization of

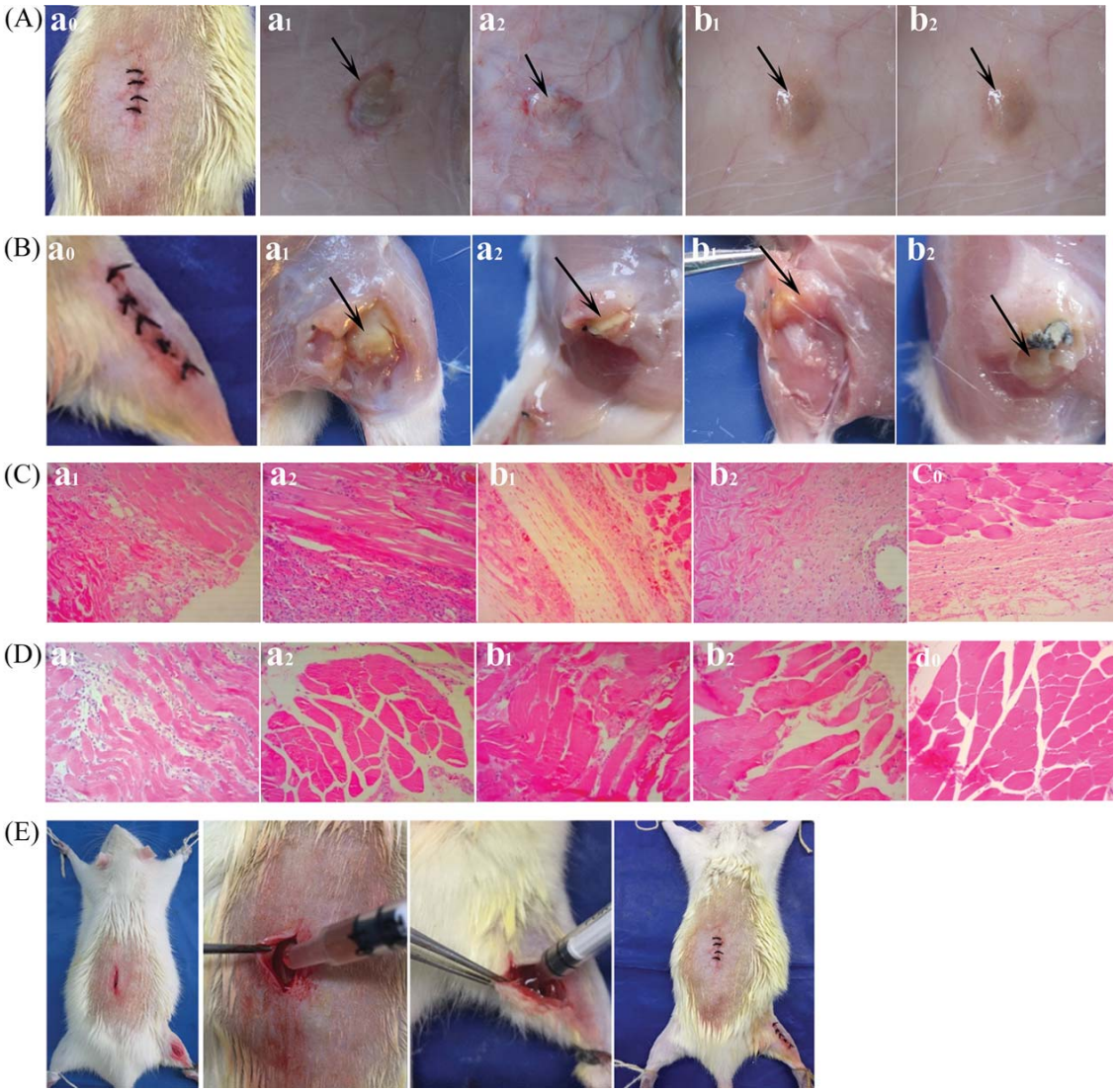

FIGURE 5. A,B: Microscopic observation of the implant site of 100 μL. (a) IO_4^--HCA-*g*-HECTS hydrogels and (b) G-IO_4^--HCA-*g*-HECTS hydrogels at (1) day 3 and (2) day 7 after implantation in (A) subcutis and (B) skeletal muscle. C,D: Histological examination of the inflammatory reaction and biodegradation of (a) IO_4^--HCA-*g*-HECTS hydrogels and (b) G-IO_4^--HCA-*g*-HECTS hydrogels at (1) day 3 and (2) day 7 after implantation in (C) subcutis and (D) skeletal muscle. (c_0) Subcutis and (d_0) skeletal muscle of normal rat as a control. (100×) The molar ratio of IO_4^- to HCA in IO_4^--HCA-*g*-HECTS hydrogels is as 0.125:1, and 20 μL genipin is added to make G-IO_4^--HCA-*g*-HECTS hydrogels. E: Surgery procedures of implanting the hydrogels into subcutaneously or into the dorsal skeletal muscle.

α, β-dehydro form of the catechol, with a maximum rate of cross-linking occurring for periodate to catechol molar ratios between 1 and 0.5. Additionally, the rate of cross-linking increases with increasing pH, due to an elevated conversion of catechol to quinone at a more basic pH values.[52]

Under the neutral conditions, our results showed that IO_4^- triggered HCA-*g*-HECTS cross-linking was highly dependent on the molar ratio of IO_4^- to catechol groups and the cross-linking temperature. As expected, the gelation time decreased obviously with the increasing molar ratio of IO_4^- to catechol and temperature because of the formation of more quinone and a faster cross-linking. In contrast to the complicated dynamic rheological properties of Fe^{3+}-HCA-*g*-HECTS, IO_4^--HCA-*g*-HECTS exhibited typical features of a covalently cross-linked elastic polymer with a frequency-independent behavior and a greater G′ than G ″. The G′ of IO_4^--HCA-*g*-HECTS hydrogel was ten-times higher than that of Fe^{3+}-HCA-*g*-HECTS hydrogel, indicating a rapid, efficient and stable cross-linking of the IO_4^- oxidized catechol groups

The adhesion strength of IO_4^- triggered HCA-g-HECTS on wet rat skin increased with a decreasing molar ratio of IO_4^- to catechol. The highest was obtained when the molar ratio of IO_4^- to catechol was 0.125:1. In this case, the balance

TABLE IV. Histological Response in Rats After Implantation of HCA-*g*-HECTS Hydrogels

	IO_4^--HCA-*g*-HECTS Hydrogel				G-IO_4^--HCA-*g*-HECTS Hydrogel			
Implant Implantation Site	Subcutis		Skeletal Muscle		Subcutis		Skeletal Muscle	
Time (days)	3	7	3	7	3	7	3	7
Number of rats examined	4	4	4	4	4	4	4	4
Capsule formation	0/4	0/4	0/4	0/4	0/4	0/4	0/4	0/4
Necrosis	0/4	0/4	0/4	0/4	0/4	0/4	0/4	0/4
Implant degradation	Slight	Marked	Slight	Marked	Slight	Marked	Slight	Marked
Inflammatory cells invasion	Marked	Marked	Marked	Slight	Moderate	Slight	Moderate	Minimal

between catechol group oxidized for cross-linking and tissue adhesion and the un-oxidized catechol for tissue adhesion made the hydrogel the best as a tissue adhesive. Double cross-linking by genipin weakened the adhesion strength of IO_4^- triggered HCA-g-HECTS possibly due to the embedding of some catechol groups in HECTS network generated by genipin, which could not contact with skin. *In vivo* adhesion evaluations showed that genipin double cross-linked IO4-HCA-g-HECTS exhibited higher adhesion strength than did the mono-cross-linked IO_4^- -HCA-g-HECTS hydrogel. The difference in adhesion strength measured *in vitro* and *in vivo* might come from the different adhesion direction in rat skin and the adhesion time. *In vitro* adhesion is between the subcutis of two pieces of rat skin, while the *in vivo* adhesion is between rat dorsum skins, newly cut through by a blade, and the skin edge containing layers of epidermis, dermis and subcutis, and blood vessels. The different interactions between hydrogel and skin may be due to the compositional differences in the skin interface. Adhesion time can also impact the adhesion strength (Table III). The adhesion time of *in vitro* and *in vivo* experiments was 24 and 48 h, respectively. This time difference can not be ignored as a factor influencing the *in vitro* and *in vivo* adhesion strengths. Interestingly, both HCA-*g*-HECTS hydrogel and double cross-linked IO_4^--HCA-*g*-HECTS hydrogel exhibit higher tensile strength in rat skin incision closure model than did the suture closure. It was noteworthy that tissue healing is a complex and dynamic process of replacing devitalized and missing cellular structures and tissue layers.[53] A combination of macroscopic and histological observations, measurements of wound healing markers, often in combination with analyses of cellular and immunologic responses should be done to evaluate the progress of wound repair in the future.

$NaIO_4$ is toxic to cells but polymer-catechol hydrogels, for example, calcium-free alginate-catechol hydrogels formed by oxidation of low concentration of $NaIO_4$ show low cytotoxicity and good biocompatibility.[25] The cytotoxicity of extract solution of IO_4^--HCA-g-HECTS hydrogel was biocompatible when the molar ratio of IO_4^- to catechol was lower than 0.5:1. *In vivo* implantation of IO_4^--HCA-g-HECTS hydrogel showed good biocompatibility as the accumulation of inflammatory

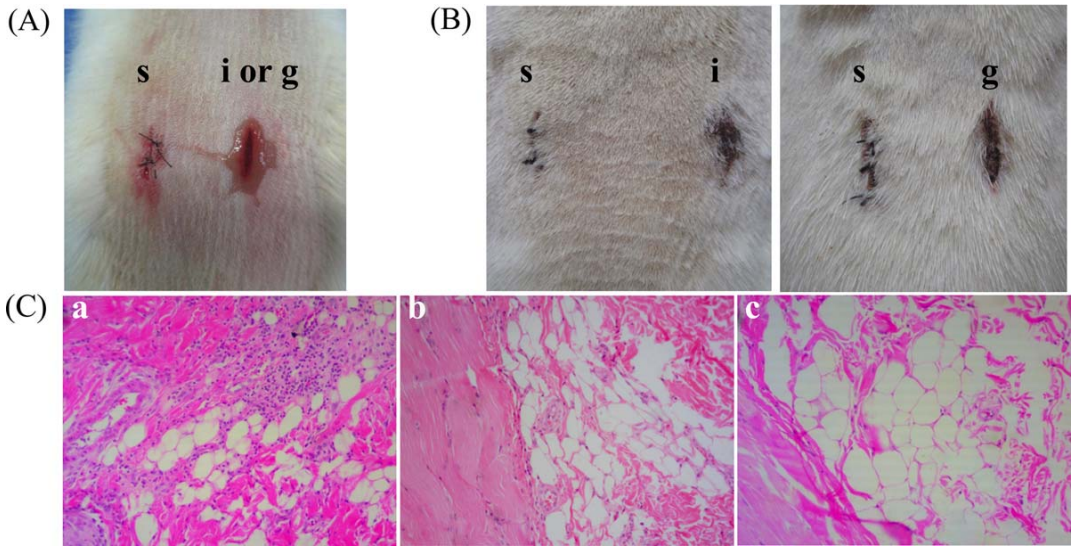

FIGURE 6. Histologic evaluation of rat skin closure. Images of rat's dorsum skin with created wounds that were closed by IO_4^--HCA-*g*-HECTS hydrogels (i), G-IO_4^--HCA-*g*-HECTS hydrogels (g) and suture (s): (A) 2 min, (B) second day postoperation. Images of hematoxylin and eosin (H&E) staining of sections of wounds at 2 days post-treatment with: (C) Control group (a), IO_4^--HCA-*g*-HECTS hydrogels (b) and G-IO_4^--HCA-*g*-HECTS hydrogels (c). (Original magnification: 100×).

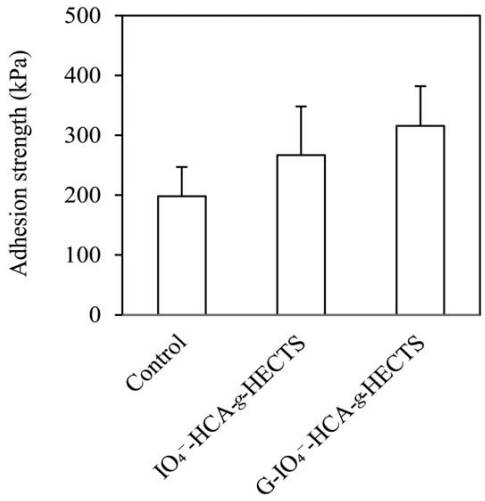

FIGURE 7. Tensile strength of healed skins closed by IO_4^--HCA-*g*-HECTS hydrogels, G-IO_4^--HCA-*g*-HECTS hydrogels and suture (control) at 48 h postoperation.

cells in the subsutis and muscle appearing on day 3 progressively decreased with time, becoming slight at day 7 post-implantation. Considering the partial absorption of HCA-g-HECTS hydrogels after one week's implantation, a longer implantation period should be designed in the future. What's more, the accumulation of inflammatory cells at the implantation site as the main tissue response to HCA-g-HECTS hydrogels should be specifically identified and calculated for a quantitative presentation of inflammation in the follow-on work.

In conclusion, the present study describes a novel biocompatible catechol conjugated hydoxyethyl chitosan. An IO_4^--triggered hydrogel of this polymer is biocompatible at the cellular level and also in tissue. This IO_4^- triggered hydrogel with molar ratio of IO_4^- to catechol as 0.125:1 exhibits an adhesion strength of 73.6 kPa on wet rat skin. At 2 days post closure, both IO_4^--triggered HCA-*g*-HECTS and double cross-linked IO_4^--HCA-*g*-HECTS hydrogels exhibit higher tensile strength in a rat skin incision closure model than do sutures. The IO_4^--HCA-g-HECTS hydrogel represents a promising tissue adhesive and warrants further investigations as an *in vivo* tissue adhesive.

REFERENCES

1. Lee BP, Messersmith PB, Israelachvili JN, Waite JH. Mussel-inspired adhesives and coatings. Annu Rev Mater Res 2011;41:99–132.
2. Hwang DS, Zeng H, Masic A, Harrington MJ, Israelachvili JN, Waite JH. Protein- and metal-dependent interactions of a prominent protein in mussel adhesive plaques. J Biol Chem 2010; 285(33):25850–25858.
3. Lin Q, Gourdon D, Sun C, Holten-Andersen N, Anderson TH, Waite JH, Israelachvili JN. Adhesion mechanisms of the mussel foot proteins mfp-1 and mfp-3. Proc Natl Acad Sci USA 2007; 104(10):3782–3786.
4. Zhao H, Robertson NB, Jewhurst SA, Waite JH. Probing the adhesive footprints of *Mytilus californianus* byssus. J Biol Chem 2006; 281(16):11090–11096.
5. Zhao H, Waite JH. Linking adhesive and structural proteins in the attachment plaque of *Mytilus californianus*. J Biol Chem 2006; 281(36):26150–26158.
6. Danner EW, Kan Y, Hammer MU, Israelachvili JN, Waite JH. Adhesion of mussel foot protein Mefp-5 to mica: An underwater superglue. Biochemistry 2012;51(33):6511–6518.
7. Wilker JJ. Biomaterials: Redox and adhesion on the rocks. Nat Chem Biol 2011;7:579–580.
8. Nicklisch SC, Waite JH. Mini-review: The role of redox in Dopa-mediated marine adhesion. Biofouling 2012;28(8):865–877.
9. Yu J, Wei W, Danner E, Ashley RK, Israelachvili JN, Waite JH. Mussel protein adhesion depends on interprotein thiol-mediated redox modulation. Nat Chem Biol 2011;7(9):588–590.
10. Wei W, Yu J, Broomell C, Israelachvili JN, Waite JH. Hydrophobic enhancement of Dopa-mediated adhesion in a mussel foot protein. J Am Chem Soc 2013;135(1):377–383.
11. Zeng H, Hwang DS, Israelachvili JN, Waite JH. Strong reversible Fe^{3+}-mediated bridging between dopa-containing protein films in water. Proc Natl Acad Sci USA 2010;107(29):12850–12853.
12. Guo Z, Ni K, Wei D, Ren Y. Fe^{3+}-induced oxidation an d coordination crosslinking in catechol–chitosan hydrogels under acidic pH conditions. RSC Adv 2015;5:37377–37384.
13. Brubaker CE, Kissler H, Wang LJ, Kaufman DB, Messersmith PB. Biological performance of mussel-inspired adhesive in extrahepatic islet transplantation. Biomaterials 2010;31(3):420–427.
14. Mirshafian R, Wei W, Israelachvili JN, Waite JH. α, β-dehydro-Dopa: A hidden participant in mussel adhesion. Biochemistry 2016;55(5):743–750.
15. Kaushik NK, Kaushik N, Pardeshi S, Sharma JG, Lee SH, Choi EH. Biomedical and clinical importance of mussel-inspired polymers and materials. Mar Drugs 2015;13(11):6792–6817.
16. Kord Forooshani P, Lee BP. Recent approaches in designing bio-adhesive materials inspired by mussel adhesive protein. J Polym Sci A Polym Chem 2017;55(1):9–33.
17. Ahn BK, Das S, Linstadt R, Kaufman Y, Martinez-Rodriguez NR, Mirshafian R, Kesselman E, Talmon Y, Lipshutz BH, Israelachvili JN, Waite JH. High-performance mussel-inspired adhesives of reduced complexity. Nat Commun 2015;6:8663.
18. Faure E, Falentin-Daudré C, Jérôme C, Lyskawa J, Fournier D, Woisel P, Detrembleur C. Catechols as versatile platforms in polymer chemistry. Prog Polym Sci 2013;38(1):236–270.
19. Sedó J, Saiz-Poseu J, Busqué F, Ruiz-Molina D. Catechol-based biomimetic functional materials. Adv Mater 2013;25(5):653–701.
20. Lee BP, Dalsin JL, Messersmith PB. Synthesis and gelation of DOPA-modified poly(ethylene glycol) hydrogels. Biomacromolecules 2002;3(5):1038–1047.
21. Ai Y, Wei Y, Nie J, Yang D. Study on the synthesis and properties of mussel mimetic poly(ethylene glycol) bioadhesive. J Photochem Photobiol B 2013;120:183–190.
22. Paez JI, Ustahüseyin O, Serrano C, Ton X-A, Shafiq Z, Auernhammer GK, d'Ischia M, del Campo A. Gauging and tuning cross-linking kinetics of catechol-PEG adhesives via catecholamine functionalization. Biomacromolecules 2015;16(12):3811–3818.
23. Park HJ, Jin Y, Shin J, Yang K, Lee C, Yang HS, Cho SW. Catechol-functionalized hyaluronic acid hydrogels enhance angiogenesis and osteogenesis of human adipose-derived stem cells in critical tissue defects. Biomacromolecules 2016;17(6):1939–1948.
24. Hong S, Yang K, Kang B, Lee C, Song IT, Byun E, Park KI, Cho SW, Lee H. Hyaluronic acid catechol: A biopolymer exhibiting a pH-dependent adhesive or cohesive property for human neural stem cell engineering. Adv Funct Mater 2013;23(14):1774–1780.
25. Lee C, Shin J, Lee JS, Byun E, Ryu JH, Um SH, Kim DI, Lee H, Cho SW. Bioinspired, calcium-free alginate hydrogels with tunable physical and mechanical properties and improved biocompatibility. Biomacromolecules 2013;14(6):2004–2013.
26. Jung YS, Jeong JH, Yook S, Im BH, Seo J, Hong SW, Park JB, Yang VC, Lee DY, Byun Y. Surface modification of pancreatic islets using heparin-DOPA conjugate and anti-CD154 mAb for the prolonged survival of intrahepatic transplanted islets in a xenograft model. Biomaterials 2012;33(1):295–303.
27. Park JY, Kim JS, Nam YS. Mussel-inspired modification of dextran for protein-resistant coatings of titanium oxide. Carbohydr Polym 2013;97(2):753–757.
28. Ryu JH, Hong S, Lee H. Bio-inspired adhesive catechol-conjugated chitosan for biomedical applications: A mini review. Acta Biomater 2015;27:101–115.

29. Cheung RC, Ng TB, Wong JH, Chan WY. Chitosan: An update on potential biomedical and pharmaceutical applications. Mar Drugs 2015;13(8):5156–5186.
30. Ryu JH, Lee Y, Kong WH, Kim TG, Park TG, Lee H. Catechol-functionalized chitosan/pluronic hydrogels for tissue adhesives and hemostatic materials. Biomacromolecules 2011;12(7):2653–2659.
31. Kim K, Kim K, Ryu JH, Lee H. Chitosan-catechol: A polymer with long-lasting mucoadhesive properties. Biomaterials 2015;52:161–170.
32. Xu J, Strandman S, Zhu JX, Barralet J, Cerruti M. Genipin-crosslinked catechol-chitosan mucoadhesive hydrogels for buccal drug delivery. Biomaterials 2015;37:395–404.
33. Ghadban A, Ahmed AS, Ping Y, Ramos R, Arfin N, Cantaert B, Ramanujan RV, Miserez A. Bioinspired pH and magnetic responsive catechol-functionalized chitosan hydrogels with tunable elastic properties. Chem Commun 2016;52(4):697–700.
34. Zhou Y, Zhao J, Sun X, Li S, Hou X, Yuan X, Yuan X. Rapid gelling chitosan/polylysine hydrogel with enhanced bulk cohesive and interfacial adhesive force: Mimicking features of epineurial matrix for peripheral nerve anastomosis. Biomacromolecules 2016;17(2):622–630.
35. Xu J, Soliman GM, Barralet J, Cerruti M. Mollusk glue inspired mucoadhesives for biomedical applications. Langmuir 2012; 28(39):14010–14017.
36. Soliman GM, Zhang YL, Merle G, Cerruti M, Barralet J. Hydrocaffeic acid-chitosan nanoparticles with enhanced stability, mucoadhesion and permeation properties. Eur J Pharm Biopharm 2014; 88(3):1026–1037.
37. Kim K, Ryu JH, Lee DY, Lee H. Bio-inspired catechol conjugation converts water-insoluble chitosan into a highly water-soluble, adhesive chitosan derivative for hydrogels and LbL assembly. Biomater Sci 2013;1:783–790.
38. Zvarec O, Purushotham S, Masic A, Ramanujan RV, Miserez A. Catechol-functionalized chitosan/iron oxide nanoparticle composite inspired by mussel thread coating and squid beak interfacial chemistry. Langmuir 2013;29(34):10899–10906.
39. Liang Y, Liu W, Han B, Yang C, Ma Q, Zhao W, Rong M, Li H. Fabrication and characters of a corneal endothelial cells scaffold based on chitosan. J Mater Sci Mater Med 2011;22(1):175–183.
40. Liang Y, Xu W, Han B, Li N, Zhao W, Liu W. Tissue-engineered membrane based on chitosan for repair of mechanically damaged corneal epithelium. J Mater Sci Mater Med 2014;25(9):2163–2171.
41. Shao K, Han B, Gao J, Song F, Yang Y, Liu W. Synthesis and characterization of a hydroxyethyl derivative of chitosan and evaluation of its biosafety. J Ocean Univ China 2015;14(4):703–709.
42. Li M, Han B, Liu W. Preparation and properties of a drug release membrane of mitomycin C with N-succinyl-hydroxyethyl chitosan. J Mater Sci Mater Med 2011;22(12):2745–2755.
43. Fan C, Fu J, Zhu W, Wang D-A. A mussel-inspired double-crosslinked tissue adhesive intended for internal medical use. Acta Biomater 2016;33:51–63.
44. Mehdizadeh M, Weng H, Gyawali D, Tang L, Yang J. Injectable citrate-based mussel-inspired tissue bioadhesives with high wet strength for sutureless wound closure. Biomaterials 2012;33(32): 7972–7983.
45. Zhang H, Bré LP, Zhao T, Zheng Y, Newland B, Wang W. Mussel-inspired hyperbranched poly(amino ester) polymer as strong wet tissue adhesive. Biomaterials 2014;35(2):711–719.
46. North MA, Del Grosso CA, Wilker JJ. High strength underwater bonding with polymer mimics of mussel adhesive proteins. ACS Appl Mater Interfaces 2017;9(8):7866–7872.
47. Caliari SR, Burdick JA. A practical guide to hydrogels for cell culture. Nat Methods 2016;13(5):405–414.
48. De Jong WH, Dormans JA, Van Steenbergen MJ, Verharen HW, Hennink WE. Tissue response in the rat and the mouse to degradable dextran hydrogels. J Biomed Mater Res A 2007;83(2):538–545.
49. De Jong WH, Eelco Bergsma J, Robinson JE, Bos RR. Tissue response to partially in vitro predegraded poly-L-lactide implants. Biomaterials 2005;26(14):1781–1791.
50. Fussell KC, Udasin RG, Smith PJ, Gallo MA, Laskin JD. Catechol metabolites of endogenous estrogens induce redox cycling and generate reactive oxygen species in breast epithelial cells. Carcinogenesis 2011;32(8):1285–1293.
51. Ghobril C, Grinstaff MW. The chemistry and engineering of polymeric hydrogel adhesives for wound closure: A tutorial. Chem Soc Rev 2015;44(7):1820–1835.
52. Cencer M, Liu Y, Winter A, Murley M, Meng H, Lee BP. Effect of pH on the rate of curing and bioadhesive properties of dopamine functionalized poly(ethylene glycol) hydrogels. Biomacromolecules 2014;15(8):2861–2869.
53. Zielins ER, Atashroo DA, Maan ZN, Duscher D, Walmsley GG, Hu M, Senarath-Yapa K, McArdle A, Tevlin R, Wearda T, Paik KJ, Duldulao C, Hong WX, Gurtner GC, Longaker MT. Wound healing: an update. Regen Med 2014;9:817–830.